Two-Dimensional Wavelength Division Demultiplexer with Surface-Normal Configuration

Jian Liu and Ray T. Chen
Microelectronics Research Center, Department of Electrical and Computer Engineering,
University of Texas at Austin, Austin, Texas 78758

Brian M. Davies and Suning Tang
Radiant Research, Inc., Austin, TX 78758

ABSTRACT

A two-dimensional wavelength-division demultiplexing device is demonstrated to seperate and to distribute optical signals of different wavelengths by use of substrate-guided wave optical interconnects. In our experiment, two stacked input holographic gratings are fabricated to steer two optical wavelengths into two different routing directions and to zigzag within a waveguiding substrate. Input coupling efficiencies of 70% and 76% are experimentally confirmed at the input wavelengths of 780 nm and 790 nm, respectively. Two arrays of 1-to-10 cascaded output holographic grating couplers are employed to couple out the optical signals with surface-normal fanouts. The crosstalk is measured to be < -30 dB. The fanout energy fluctuation is within ± 10% for each wavelength.

Key words: Wavelength division multiplexing; Volume hologram; Optoelectronic interconnects; Network; Photopolymer films.

1. Introduction

Wavelength-division (de)multiplexer (WD(D)M) is a pivotal bandwidth enhancement component in optical fiber communications and optical sensor systems. Various types of optical WD(D)M have been proposed and demonstrated.[1-13] These include gratings[1], thin film filters[2], fused-fiber coupler[3], waveguide-type[4,5], Bragg-reflector-in-fiber devices[6], Febry-Perot interferometer-type filters[7], holographic optical element (HOE) based transmission-type demultiplexers[8-10], and polarization-independent optical filters[11-13]. These approaches can only be used for wavelength filtering or seperation. When the WDDMs are applied to the fiber-to-home network[14] or multi-sensors system[15], it is nessecerry for them to be able to route seperate wavelength channels and to distribute each channel to many users.

Photopolymer-based substrate guided wave optical interconnects, using photopolymer volume holograms combined with total internal reflection (TIR) in waveguiding substrates, have been demonstrated as efficient approaches for intra- and inter-module interconnections, optical clock distributions, optical backplane buses, and optical networks[16-18]. In this paper, by means of photopolymer-based substrate guided wave optical interconnects, a two-dimensional (2-D) WDDM serving the functions of wavelength

seperation and 1-to-many fanouts is demonstrated. In our design, stacked volume holograms are employed as the input couplers to steer input optical signals with different wavelengths to their desired directions, and then coupled-out by output HOE arrays. This two-dimensional network configuration having both the input and output HOEs integrated on one waveguiding plate fulfills simultaneously wavelength seperation, routing, and optical signal distribution. Experimental results of routing and distributing two optical channels at wavelengths of 780 nm and 790 nm are presented.

2. Design of a two-dimensional WDDM network

Figure 1(a) shows a schematic diagram for a two-dimensional WDDM network. The input and the output volume holograms are integrated on the same waveguiding substrate at their designated positions. Two stacked volume holograms are used as the optical wavelength routing filters to couple two input optical signals λ_1 and λ_2 into their designed routing directions with an angle of $90^\circ - \alpha$ between them in XY plane as indicated in Figure 1(b). The bouncing angle within the waveguiding substrate is greater than the critical angle of the substrate. The two stacked volume holographic gratings and their phase matching diagrams are given in Figure 1 (b), in which the input wave vector $\mathbf{k_1}$ ($|\mathbf{k_1}| = 2\pi n / \lambda_1$) is phase-matched with the grating vector $\mathbf{K_1}$ ($|\mathbf{K_1}| = 2\pi / \Lambda_1$), and so does the $\mathbf{k_2}$ ($|\mathbf{k_2}| = 2\pi n / \lambda_2$) and the $\mathbf{K_2}$ ($|\mathbf{K_2}| = 2\pi / \Lambda_2$). n is the average refractive index of the holographic medium. The angle between the two projected grating vectors in XY plane is $90^\circ - \alpha$. The separated optical signals propagate within the waveguiding substrate with total internal reflection and are distributed to their respective destinations, and then coupled out surface-normally by the two arrays of cascaded volume holograms at the surface-normal direction. Many users may share the same source with this distributed 2-D WDDM. It is promising for this two-dimensional configuration to be used for filtering and distributing wavelength channels centered at 0.8 μm, 1.3 μm and 1.55 μm. It is also possible to realize multiple-wavelength channels seperation and distribution by stacking more input holographic gratings and by integrating more arrays of output couplers at the desired wavelengths and positions. To get a small channel wavelength spacing, it is important to fabricate the input couplers with a narrow bandwidth, and to make the output couplers capable of accomodating a larger angular deviation to couple the optical signal out of the waveguiding plate.

Figure 2(a) shows a transmission volume hologram with an input optical signal incident at an angle of θ with respect to the surface normal direction. For a typical substrate guided wave optical interconnect with the surface-normal configuration, the diffraction angle of the volume hologram is designed to be 45° in a quartz substrate while optical signal is incident from the surface-normal direction with $\theta = 0$. The deviation of operating wavelengths and the incident angle θ are evaluated using coupled wave theory[19]. Figure 2(b) shows the simulation results of diffraction efficiencies versus the wavelength deviation from central wavelength 780 nm and 790 nm of an s-wave with refractive index n = 1.52 for DuPont photopolymer

films. The film thickness is 100 μm. The corresponding refractive index modulation Δn is determined to be 0.0033 for a 100% diffraction efficiency at 790 nm. From Figure 2(b), we can see that the 3dB bandwidths (full width at half maximum (FWHM)) is 8 nm for the 100 μm thick film. Figure 3 shows the diffraction efficiencies as a function of the incident angle deviation at 790 nm (similar results are obtained at 780 nm). The parameters used are same as those in Figure 2(b) except that Δn = 0.0166 for 20 μm thick film. The angle deviation tolerances at half maximum of the diffraction efficiency are 1.7^{o} and 0.4^{o}, respectively. To demultiplex and distribute two wavelength channels at 790 nm and 780 nm, we employ 100 μm thick films as input wavelength channel routing filters and 20 μm thick films as the output coupler arrays.

3. Experiment

In our experiment, An Argon ion laser operating at 514 nm is used to record volume hologram. A Ti: Sapphire tunable laser is employed to carry out the measurement. To demonstrate the conceptual two-dimensional WDDM network shown in Figure 1(a), we choose Dupont photopolymer HRF 150 with 100 μm film thickness as the input holographic grating couplers. Two stacked holographic films are sequentially laminated on a quartz plate. The thickness of the substrate is d' = ~ 1.6 mm. The bouncing angle within the substrate is 45^{o}. The angle between the two routing directions is designed to be $\sim 45^{o}$. One holographic grating is designed to deflect optical signal at λ_1 = 790 nm, and the other is for λ_2 = 780 nm. Two arrays of output holographic grating couplers are also fabricated along the desired routing direction for reconstruction wavelength at 780 nm and 790 nm, respectively, by employing DuPont photopolymer film HRF 600 with a 20 μm film thickness. By taking advantage of the fact that the collimated laser beam is with a Gaussian intensity profile during hologram recording, we are able to record the output couplers with relatively uniform fanout distribution for both arrays.

Figure 4(a) shows the experimental results when the device operates at 780 nm and 790 nm simultaneously. The diffraction efficiencies of the input holographic grating couplers are measured to be 70% and 76%, respectively. The 3dB angular deviations of the volume holograms are measured to be within 0.5^{o}. The two wavelengths are succesfully separated and directed to their designed directions by the two stacked input holographic grating coupler. Each wavelength channel has ten fanouts. The energy distribution non-uniformity is measured to be within ± 10%. Figure 4(b) shows a combined output spectra of 780 nm and 790 nm. The crosstalks between two channels are measured to be smaller than -30dB. It is obvious that this two-dimensional network configuration provides a robust, reliable, surface-mountable, and cost-efficient device with combined functions of wavelength demultiplexing and distributing.

4. Conclusion

In conclusion, we demonstated a cost-efficient and user-sharing two-dimensionanal wavelength demultiplexing and distributing optical network, with which optical signals at 790 nm and 780 nm are seperated and diffracted into the waveguiding plate in two different routing directions by two stacked DuPont holographic gratings with a 100 μm thickness, distributed within the glass substrate with total internal reflection, and coupled out of the substrate to each user by output holographic grating with 20 μm thickness. By using two different kinds of photopolymer films, we may obtain narrow band filtering function for input couplers and large angular tolerance for output couplers. The crosstalks are measured to be <-30dB, and the non-uniformity of the fanout energy distribution is within ± 10%. The relatively uniform fanout energy distribution is pivotal to the integration with photodetector arrays for practical system designs. The monolithic integration of the input and output couplers on a waveguiding substrate provides a robust architecture against environmental and mechanical perturbations. Furthermore, it is possible to realize multi-wavelength channels routing and distribution involving 0.8 μm, 1.3 μm and 1.55 μm wavelengths. by stacking holographic gratings as input wavelength seperating and routing couplers and by integrating arrays of output couplers at desired wavelengths.

Acknowledgments: This research is supported by Ballistic Missile Defence Organization, Army SSDC, the Center of Optoelectronics Science and Technology (COST), Office of Naval Research, Cray Research, DuPont, Lightpath, and the Advanced Technology Program (ATP) of the state of Texas.

References:

1. M. Seki, K. Kobayashi, Y. Odagiri, M. Shikada, T. Tanigawa, and R. Ishikawa, "20-channel micro-optic grating demultiplexer for 1.1-1.6 μm band using a small focusing parameter graded-index rod lens," Electron. Lett. **18**, 257-258 (1982).
2. K. Nosu, H. Ishio, and K. Hashimoto, "Multireflection optical multi/demultiplexer using interference filters," Electron. Lett. **15**, 414-415 (1979).
3. C. M. Lawson, P. M. Kopera, T. Y. Hsu, and V. J. Tekippe, "In-line single-mode wavelength division multi/demultiplexer," Electron. Lett. **20**, 963-964 (1984).
4. B. H. Verbeek, C. H. Henry, N. A. Olsson, K. J. Orlowsky, R. F. Kazarinov, and B. H. Johnson, "Integrated four-channel Mach-Zehnder multi/demultiplexer fabricated with phosphorous doped Si_iO_2 waveguides on S_i," IEEE J. Lightwave Technol. 6, 1011-1013 (1988).

5. C. Dragone, "An NxN optical multiplexer using a planar arrangement of two star couplers," IEEE Photon. Technol. Lett. **3**, 812-814 (1991).
6. W. S. Whalen, M. D. Divino, and R. C. Alferness, "Demonstration of a narrowband Bragg-reflection filter in a single-mode fiber directional coupler," Electron. Lett. **22**, 681-682 (1986).
7. K. H. Hirabayashi, H. Tuda, and T. Kurokawa, "Narrow-band tunable wavelength-selective filters of Fabry-Perot interferometers with a liquid crystal intracavity," IEEE Photon. Technol. Lett. **3**, 213-215 (1991).
8. A. L. Dmitriev and A. V. Ivanov, "Holographic element of a demultiplexer for a lightguide communication system," Opt. Spectrosc. **62**, 91-93 (1987).
9. J. L. Horner and J. E. Ludman, "Single holographic element wavelength demultiplexer," Appl. Opt. **20**, 1845-1847 (1981).
10. M. M. Li and R. T. Chen, "Five-channel surface-normal wavelength-division demultiplexer using substrate-guided waves in confunction with a polymer-based littrow hologram," Opt. Lett. 20, 797-799 (1995).
11. C. Wu, C-M Wu, D. G. Knight, C. Blaauw, N. Puetz, F. Shepherd, G. Rabikovs, and K. D. Chik, "Novel polarization independent tunable optical filter with yield compensation after fabrication," Electron. Lett. **31**, 231-232 (1995).
12. X. Fu and J. M. Xu, "A novel grating-in-etalon WDM device and a proof-of-concept demonstration of a 1x40 polarization insensitive WDM," IEEE Photon. Technol. Lett. **9**, 779-781 (1997).
13. A. N. Starodumov, L. A. Zenteno, D. Monzon, and A. R. Boyain, "All-fiber polarization-independent narrow band wavelength-division multiplexer," Opt. Comm. **138**, 31-34 (1997).
14. I. P. Kaminow and T. L. Koch, *Optical Fiber Telecommunications IIIA*, Academic Press, New York (1997).
15. R. T. Chen, D. Robinson, H. Lu, M. R. Wang, T. Jannson, and R. Baumbick, "Reconfigurable optical interconnection network for multimode optical fiber sensor arrays," Opt. Eng. **31**, 1098-1105 (1992).
16. R. T. Chen, C. Zhou, C. Zhao, and R. Lee, "Photopolymer-based waveguide holograms for optoelectronic interconnects applications," Critical Rev. Optical Sci. Technol. **CR-63**, 46-64 (1996).
17. Jian Liu, Chunhe Zhao, R. Lee, and Ray T. Chen, "Cross-link optimized cascaded volume hologram array with energy-equalized one-to-many surface-normal fan-outs," Opt. Lett. **22**, 1024-1026 (1997).
18. Jian Liu, Chunhe Zhao, and Ray T. Chen, "Implementation of optical perfect shuffle with substate-guided wave optical interconnects," IEEE Photon. Technol. Lett. **9**, 946-948 (1997).
19. H. Kogelnik, "Coupled wave theory for thick hologram gratings," The Bell Sys. Tech. J. **13**. 2909-2947 (1969).

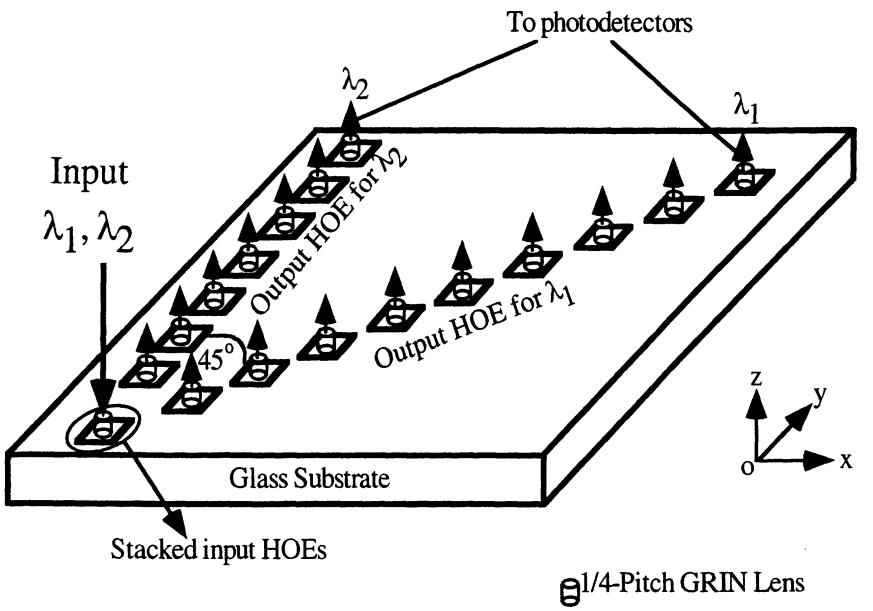

(a)

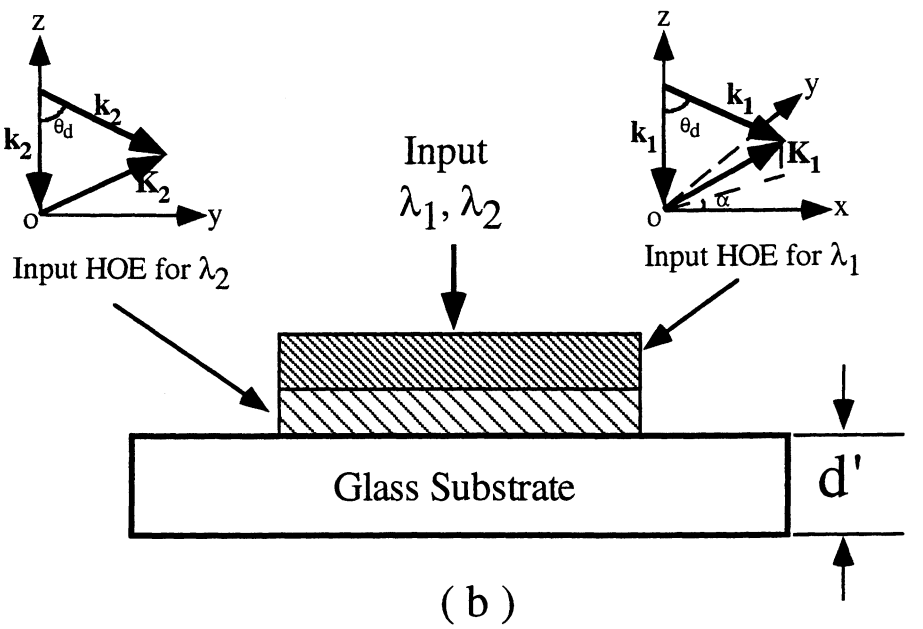

(b)

Figure 1 (a) Schematic diagram of a two-dimensional WDDM; (b) two stacked volume holographic input couplers and their phase matching diagrams.

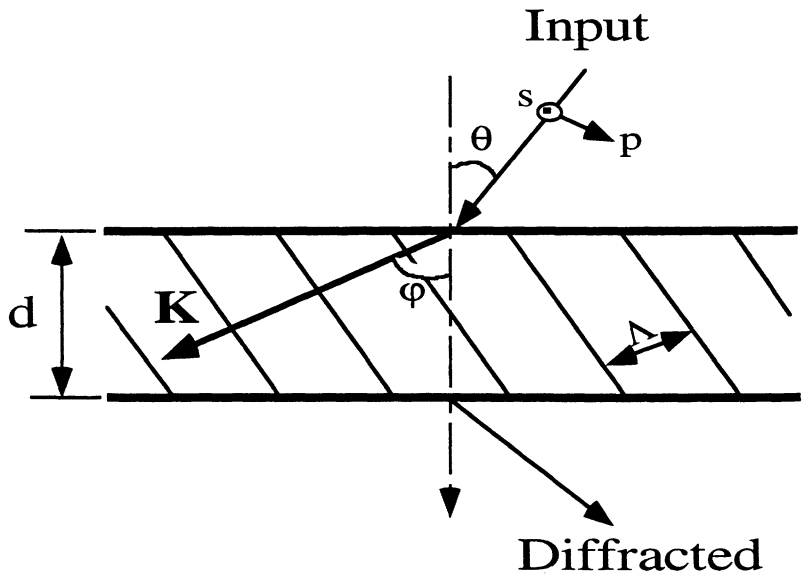

(a)

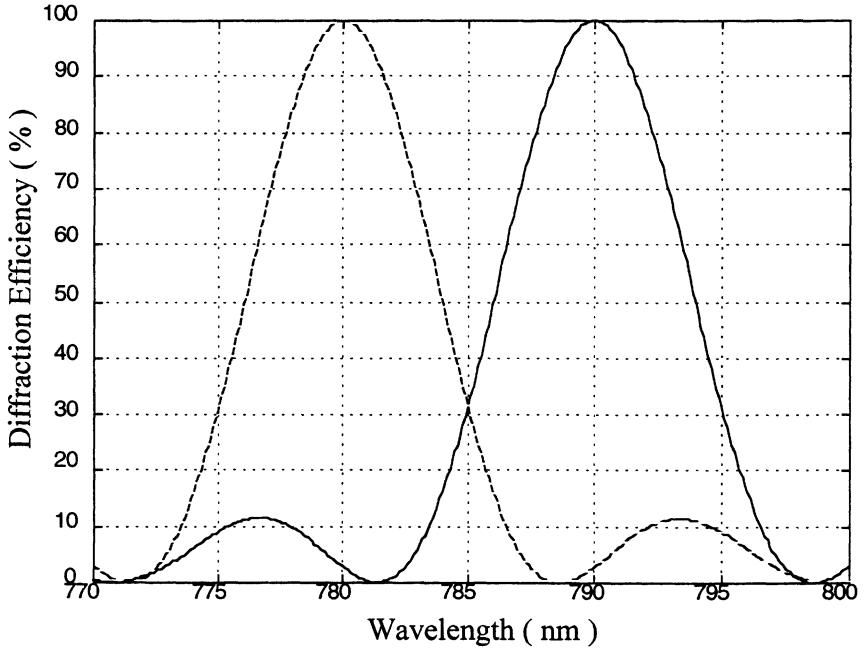

(b)

Figure 2 (a) A transmission volume hologram; (b) simulation results of diffraction efficiencies versus the wavelength deviation from central wavelengths 780nm and 790 nm of an s-wave.

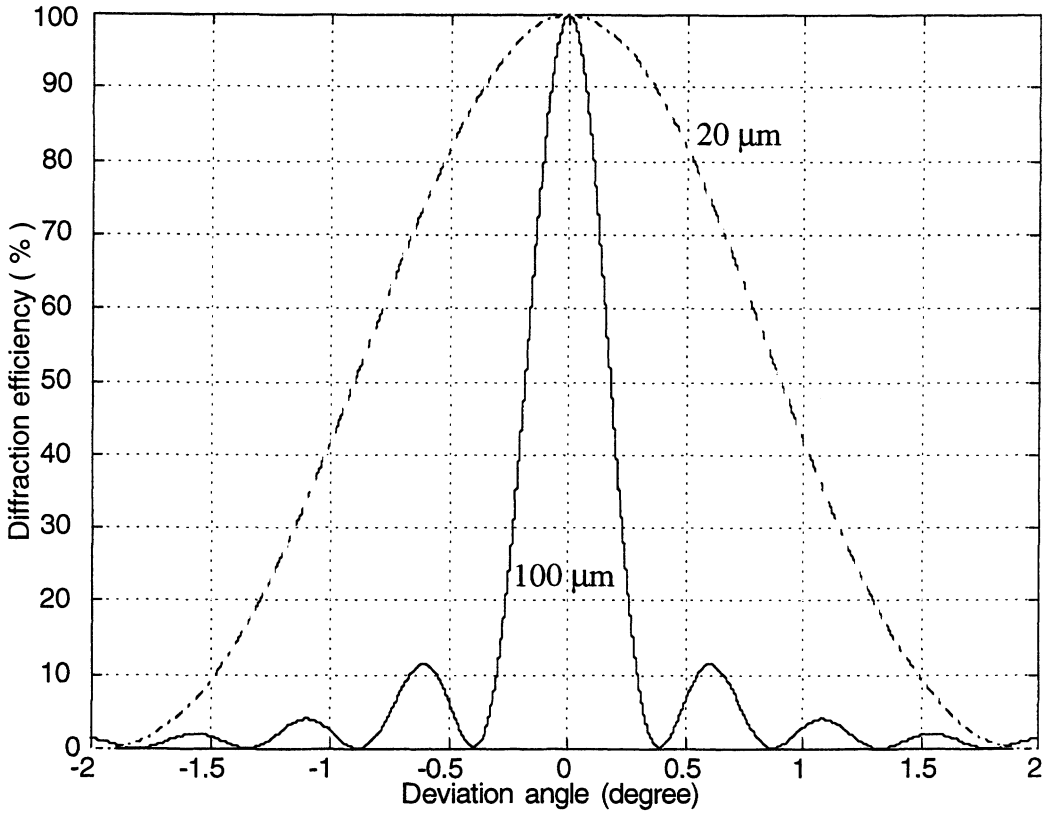

Figure 3 Diffraction efficiencies versus the incidence angle deviation at 790 nm. Similar results are obtained for 780 nm.

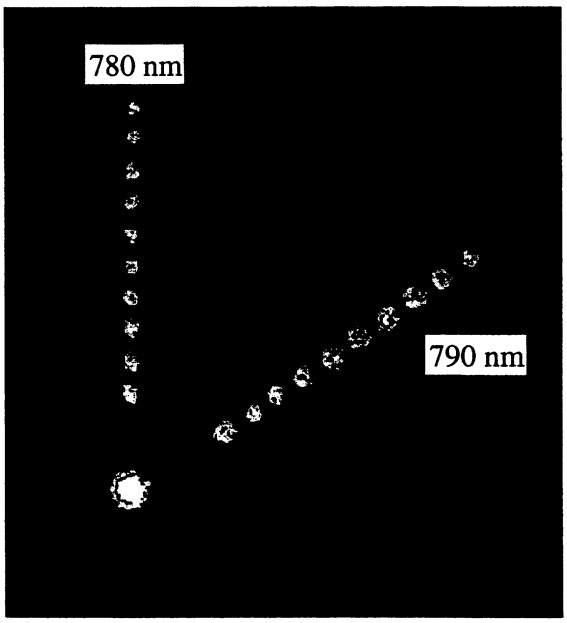

(a)

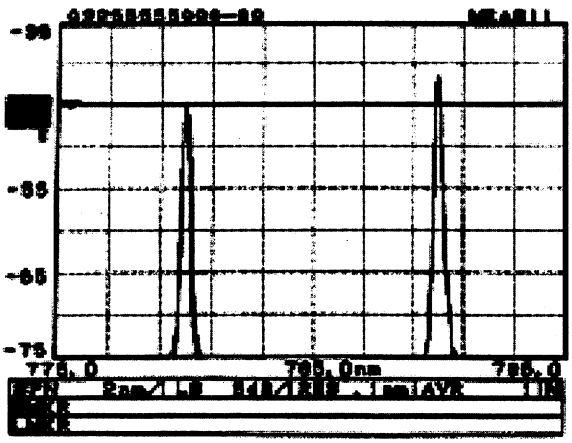

(b)

Figure 4 (a) Experimental results of the two-dimensional WDDM device while operating at 790 nm and 780 nm. (b) combined output spectra of the first spots of 780 nm channel and 790 nm channel.